Journal of Medicinal Chemistry

Article

Rational design of calpain inhibitors based on calpastatin peptidomimetics

Kristin E. Low, Spencer Ler, Kevin Chen, Robert Laurence Campbell, Jennifer L. Hickey, Joanne Tan, Conor C. G. Scully, Peter L. Davies, Andrei K Yudin, and Serge Zaretsky

J. Med. Chem., **Just Accepted Manuscript** • DOI: 10.1021/acs.jmedchem.6b00267 • Publication Date (Web): 05 May 2016

Rational design of calpain inhibitors based on calpastatin peptidomimetics

Kristin E. Low,[1] Spencer Ler,[2] Kevin Chen,[1] Robert L. Campbell,[1] Jennifer L. Hickey,[3] Joanne Tan,[2] Conor C. G. Scully,[2] Peter L. Davies,[1]* Andrei K. Yudin,[2]* and Serge Zaretsky[2]*

[1]Department of Biomedical and Molecular Sciences, Queen's University, Kingston, ON, K7L 3N6, Canada

[2]Department of Chemistry, University of Toronto, Toronto, ON, M5S 3H6, Canada

[3]Encycle Therapeutics Inc., 101 College Street, Suite 314, Toronto, Ontario M5G 1L7, Canada

Abstract

Our previously reported structures of calpain bound to its endogenous inhibitor calpastatin have motivated the use of aziridine aldehyde-mediated peptide macrocyclization towards the design of cyclic peptides and peptidomimetics as calpain inhibitors. Inspired by nature's hint that a β-turn loop within calpastatin forms a broad interaction around calpain's active site cysteine, we have constructed and tested a library of 45 peptidic compounds based on this loop sequence. Four molecules have shown reproducibly low micromolar inhibition of calpain-2. Further systematic sequence changes led to the development of probes that displayed increased potency and specificity of inhibition against calpain over other cysteine proteases. Calculated K_i values were in the low μM range, rivaling other peptidomimetic calpain inhibitors and presenting an improved selectivity profile against other therapeutically relevant proteases. Competitive and mixed inhibition against calpain-2 was observed and an allosteric inhibition site on the enzyme was identified for a non-competitive inhibitor.

Keywords

cyclic peptide; calpain; calcium-activated protease; inhibitor; enzyme kinetics; cysteine protease; macrocycles

Introduction

Calpains are a family of Ca^{2+}-activated cytosolic multi-domain cysteine proteases that are responsible for specific, limited cleavage of a wide variety of proteolytic targets.[1] They act on

Ca^{2+} signals to bring about cellular responses such as reorganization of the cytoskeleton, cell cycle regulation, and apoptosis.[2-4] Over-activation, either by specific mutations or upstream effects, cause numerous pathological conditions in heart attack, stroke, Alzheimer's disease, cancer, neurodegeneration, muscular dystrophy, and traumatic brain injury.[4-8]

The most extensively studied isoforms, calpains-1 and -2, are heterodimers composed of an isoform-specific 80-kDa large subunit and a common 28-kDa small subunit.[1,3,5,9-13] Calpain-1 requires multi-μM concentrations of Ca^{2+}, while calpain-2 requires an order of magnitude higher level in the sub-mM range. [14-20] Activation by Ca^{2+} induces conformational changes in the enzyme, aligning the domains of the protease core for active site cleft formation and resulting in an overall more compact enzyme.

Calpains-1 and -2 have a highly specific natural inhibitor, calpastatin, which is thought to limit their proteolytic activity within the cell. Calpastatin binds the enzyme only when the latter is in the Ca^{2+}-activated form and is released from the enzyme at low concentrations of Ca^{2+}.[21,22] Calpastatin is an intrinsically unstructured 70-kDa protein comprised of five domains, four of which (CAST 1 through 4) are homologous and independently inhibitory and each contain subdomains A, B, and C.[2,23] Crystal structures of Ca^{2+}-bound calpain inhibited by calpastatin have revealed the mode of inhibition.[15,17,24] Subdomains A and C, which help anchor the inhibitor to the enzyme (Figure 1), form amphipathic α-helices upon binding to hydrophobic clefts in the two penta-EF hand (PEF) domains. Subdomain B is responsible for inhibition of calpain by binding and occluding the primed and unprimed sides of the active site cleft formed by the protease core domains. Subdomain B avoids cleavage by looping out and away from the active site cysteine with a β-turn at the conserved Lys_{611}-Leu_{612}-Gly_{613}-Glu_{614}. It also forms a two-turn amphipathic α-helix that binds on the primed side of the cleft.

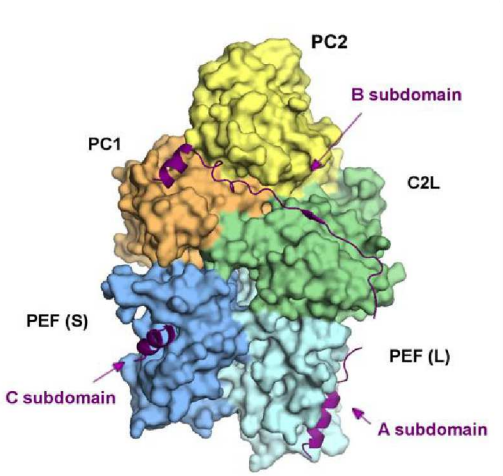

Calpain's many roles in the cell and involvement in a variety of physiological conditions and diseases clearly identifies the protease as a potential therapeutic target.[5,9,11] Calpain inhibitors display a wide range of potency but, to date, have not been specific enough to avoid inhibiting other cysteine proteases such as cathepsins.[5,25,26] While there are many types of calpain inhibitors, including active site directed reversible and irreversible inhibitors[25,26] with various reactive warheads, their gains in efficacy have not supplanted the need for specificity. Many probes such as E64 and the peptidomimetic epoxide based WRH(*R*,*R*) class of compounds are only marginally calpain specific and affect a broad range of cysteine proteases.[27] Attempts to increase selectivity of many compounds with more calpain specific warheads have often decreased potency.[26] The di and tripeptides designed by Tripathy *et al.* were demonstrated to be

highly potent with moderate selectivity, but lack therapeutic potential due to their low aqueous solubility.[28] In their work on ketoamide inhibitors of calpain, AbbVie noted pharmacokinetic issues in development due to poor cellular stability.[29,30] Moreover, as the physiological targets of calpain cleavage remain largely undefined, calpain-selective inhibitors are sought for their use as *in vitro* tools for target identification in addition to use against aforementioned calpain-associated pathologies. Calpain isoform specificity is also desired in cases of isoform-specific pathologies. Currently, most compounds show marginal selectivity between calpains-1 and -2, which can prevent progression into clinic trials of such compounds, such as seen with *N*-(4-fluorophenylsulfonyl)-l-valyl-l-leucinal, SJA-6017.[31,32]

The recent crystal structures of Ca^{2+}-activated calpain have allowed for the structure-based design of inhibitors along the entire active site cleft, including those regions of potential interaction with the calpain-specific C2-like (C2L) domain.[15,17] This had not been possible before, as the only structures available of calpain in the active conformation were those of the uninhibited and inhibited protease core (PC) (domains PC1 + PC2).[14,16,18-20]

Proteases universally bind to the extended β-strand conformation of their substrates.[33] This insight provides a possible explanation for the superior inhibition achieved by many peptidomimetic molecules with conformational restrictions that favour a β-strand-like formation.[24,34] Similar trends have been noted for calpain inhibition.[26] Since recognition sequences are often 4-5 residues in length, one successful approach to inhibitor synthesis is to lock the sequence into a specific conformation within a cyclic peptide. Cyclization can result in a reduced entropic penalty for binding to a protein host, thereby making it a favourable interaction.[35,36] In addition, cyclic peptides exhibit greater stability to proteolytic degradation by peptidases in the cell.[37] Cyclic peptides have previously been used to successfully inhibit HIV

protease,[21] HCV NS3 protease,[23] and even calpain (Figure 2).[24] To further capitalize on the cyclization β-strand locking mechanism, we noted that calpastatin has a conserved β-turn where it binds to the active site of calpain.

We hypothesized that by using the calpain-specific inhibition characteristics of calpastatin, we would be able to design novel, potent calpain inhibitors. Specifically, inhibitor design based on the calpastatin β-turn residues KLGE would propagate calpastatin-like specificity and potency to such inhibitors. Designing inhibitors in this manner without a chemical warhead would allow to avoid the high potential for toxicity found with compounds containing reactive centers, thus potentially improving clinical use.[26] Based on prior work with cyclic peptides derived from aziridine aldehyde-mediated peptide macrocyclization, we expected 18-membered rings to adopt rigid β -turn structures. Additionally, we were interested in comparing the structure-activity effects of constraining the KLGE-type sequences within cyclic peptides to amidine-based cycle-tail motif peptidomimetics that are also derived from the aziridine aldehyde-mediated macrocyclization chemistry (Figure 2). Here, we show that cyclic peptide and amidine-based cycle-tail motif peptidomimetics inhibit cysteine proteases, including calpain, and that both show various modes of inhibition of calpain-2 with K_i values in the low micromolar range. In addition, photo-reactive cross-linking has been used to identify inhibitor binding sites for two of the library compounds.

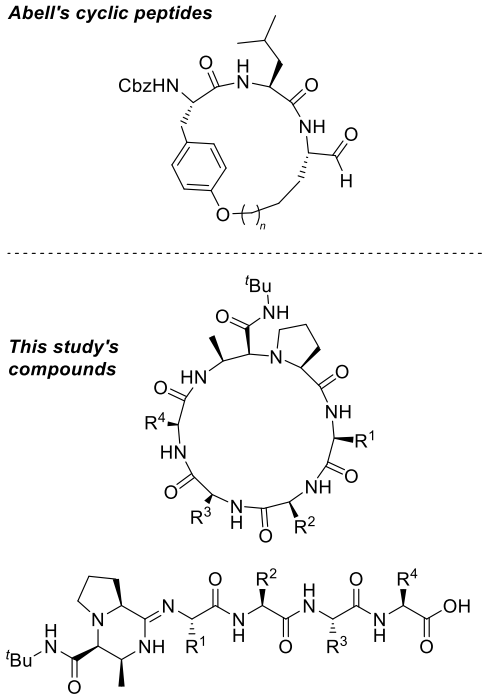

Figure 2. Comparison of Abell's cyclic peptide inhibitors of calpain[24] to compounds from this study, which were derived from the multicomponent synthesis of peptides, aziridine aldehydes, and isocyanides

Experimental Section

Materials. Active wild-type and inactive C105S mutant rat recombinant calpain-2,[38] and rat calpain-1 protease core[14] were expressed and purified as previously described. Rat calpain enzymes were used over human-sourced calpains based on the availabilities of recombinant expression techniques for high quantities of protein, and the crystal structures of rat full-length enzyme and protease core construct. Papain, human cathepsin L, the cysteine protease substrate

Z-FR-AMC, and leupeptin were purchased from Calbiochem. The calpain substrate (EDANS)-EPLFAERK-(DABCYL) was synthesized by Biomer Technology.

Cyclic peptide and peptidomimetic synthesis. Peptides were synthesized using the telescopic cyclization/aziridine ring-opening synthesis.[39] Unless otherwise noted, a Pro-terminated peptide was cyclized at a 0.10 mmol scale in a 2-dram vial. To it, was added aziridine aldehyde dimer (0.10 mmol, 2.0 eq. as monomer), TFE (1.0 mL, 0.1 M), and *tert*-butyl isocyanide (0.2 mmol, 2.0 eq.). The reaction was left to stir at room temperature for 4 h and monitored throughout by RP-HPLC/MS. Ring-opening of the aziridine moiety was initiated by addition of thiobenzoic acid (0.4 mmol, 4.0 eq) and left to stir for 2 more hours. Afterwards, Raney®-Nickel slurry (approx. 1.5 mL) was added, reaction capped, and allowed to stir for a final 16 h. The mixture was filtered through Celite with methanol, and concentrated under reduced pressure. TFA/DCM (1:1, 4 mL) was then added to the mixture to deprotect the side chains. The cleavage cocktail was evaporated with a stream of nitrogen after 2 h of stirring at room temperature. The TFA salt was then purified by semi-preparative RP-HPLC/MS or reversed-phase flash chromatography. The pure fractions were pooled together and lyophilized to afford the final products as white or off-white powders. Purity was confirmed to be ≥ 95% by HPLC/MS and products were identified by NMR and HPLC/MS (see the Supporting Information).

RP-HPLC/MS. Low resolution mass spectra (ESI) were collected on an Agilent Technologies 1200 series HPLC paired to a 6130 Mass Spectrometer. Compounds were resolved on an Agilent Poroshell 120 EC-C_{18}, 2.7 μm, 4.6 x 50 mm^2 column at room temperature with a flow of 1 mL/min. The gradient consisted of eluents A (0.1% formic acid in double-distilled water) and B

(0.1% formic acid in HPLC-grade acetonitrile). The gradient method started with a step of 5% of B for the first 0.99 min, followed by a linear gradient from 5% to 95% B in 8.0 min. The column was then washed with 95 % B for 1.0 min and equilibrated at 5% B for 1.5 min.

Peptide NMR. ^{1}H and ^{13}C NMR spectra were recorded on Varian Mercury 400 and Agilent 500 MHz or 600 MHz spectrometers. ^{1}H NMR spectra were referenced to $CDCl_3$ (7.26 ppm), CD_3OD (3.30 ppm), DMSO-d_6 (2.50 ppm). ^{13}C NMR spectra were referenced to $CDCl_3$ (77.2 ppm), CD_3OD (49.0 ppm), and DMSO-d_6 (39.52 ppm). NMR spectra were recorded at 25 °C unless otherwise specified. Peak multiplicities are designated by the following abbreviations: s, singlet; bs, broad singlet; d, doublet; t, triplet; q, quartet; m, multiplet; ds, doublet of singlets; dd, doublet of doublets; ddd, doublet of doublet of doublets; bt, broad triplet; td, triplet of doublets; tdd, triplet of doublets of doublets.

Modelling, docking simulation, and molecular dynamics simulation studies. Initial designs for the cyclic peptides were modelled using PyMOL based on the crystallographic structure of calpastatin-bound calpain-2 (PDB: 3BOW).[15] SBGrid Consortium-supported software applications were used.[40] Molecular dynamics (MD) calculations were done with the GROMACS package[41] on calpain-2. The protein was solvated in a box using 30365 water molecules. The net charge of the system was neutralized with 18 sodium ions. The system was then subjected to energy minimization, position-restrained molecular dynamics to settle the water molecules, and unrestrained molecular dynamics simulations. The simulations were run at a temperature of 273 K using a time step of 2 fs for a total duration of 20 ns. Long-range electrostatics were treated with the particle mesh Ewald method. The simulations were conducted

under isothermal conditions using V-rescale temperature coupling. MD studies with calpain-2 used the CHARMM[42] and OPLS[43] force fields for protein and the SPCE water model. MD calculations were also done on select cyclic peptides. Topology files and parameters for the cyclic peptides were provided by SwissParam.[44] MD studies with cyclic peptides were run in a similar method to those of calpain-2 and used the CHARMM force field.[42] Results were analyzed using VMD.[45] Docking simulations were done using AutoDock4 and AutoDockTools4,[46] and Glide[47-49] in the Maestro Schrödinger Software Suite for docking the cyclic peptides to the active site cleft of calpain-2, calpain-1 protease core, and papain. The protein receptors were used in rigid docking mode. For the cyclic ligands, residue side chains maintained flexibility while the peptide backbone was torsionally constrained based on NMR structures. The AutoDock4 dockings were performed using the Lamarckian genetic algorithm with parameters as follows: 100 dockings, population size of 150, random starting position and conformation, translation steps of 2.0 Å, rotation steps of 50°, mutation rate of 0.02, crossover rate of 0.8, local search frequency of 0.06, and 2.5 million energy evaluations. Final docked conformations were clustered using a root-mean-squared deviation (RMSD) of 2.0 Å. Glide dockings were performed using default settings with some exceptions: Glide-XP (extra precision) option was selected, torsional constraints were set for cycle backbone and peptide bonds starting from the compound's NMR structure, and at most 100 poses per ligand were produced. Glide docking results were analyzed by Prime MM-GB/SA[50,51] to determine the free energies of binding.

Peptide inhibitor library screening and calpain inhibition kinetics using a fluorescence-based hydrolysis assay. The rate of cleavage of the (EDANS)-EPLFAERK-(DABCYL) fluorescent

substrate was monitored in a 0.5-mL cuvette using a Perkin-Elmer LS55 fluorescence spectrometer with λ_{ex} = 335 nm, λ_{em} = 500 nm and slit widths of 10 nm. Triplicate readings were obtained at 0.1 s intervals. The cuvette contained 100 nM rat calpain-1 protease core or 10 nM rat calpain-2, 5 μM substrate, and 1-100 μM peptide inhibitor (dissolved in DMSO at stock concentrations of 50 mM) in 10 mM HEPES (pH 7.4) and 10 mM DTT. Control assays were performed with an equivalent amount of DMSO. The total concentration of DMSO in each reaction was 0.4%. The reaction was initiated with the addition of $CaCl_2$ to 4 mM in a final volume of 0.5 mL.

Inhibition of papain and cathepsin L in a fluorescence-based hydrolysis assay. For papain activity assays, the rate of cleavage of the (EDANS)-EPLFAERK-(DABCYL) fluorescent substrate was measured in a similar manner as the calpain activity assays. For human cathepsin L activity assays, the rate of cleavage of the Z-FR-AMC fluorescent substrate was quantified again in a similar manner but with λ_{ex} = 360 nm, λ_{em} = 460 nm and slit widths of 8 nm. Triplicate readings were obtained at 0.1 s intervals. The cuvette contained 5 μM (EDANS)-EPLFAERK-(DABCYL) or 5 μM Z-FR-AMC, and 100 μM peptide inhibitor (dissolved in DMSO at stock concentrations of 50 mM) in 10 mM HEPES (pH 7.4) and 10 mM DTT (papain) or 0.1 M NaOAc-HCl (pH 5.5), 1 mM EDTA, and 1 mM DTT (cathepsin L). Control assays were performed with an equivalent amount of DMSO. The total concentration of DMSO in each reaction was 0.4%. The reactions were initiated by the addition of 30 nM papain or 1 nM cathepsin L, respectively. The initial rates were determined according to the procedure used for the calpain activity assay. All reactions were performed at 298 K.

Analysis of enzyme kinetics with lead compounds. Fluorogenic hydrolysis assays were performed with concentrations of substrate ranging from 1-100 μM and inhibitor concentrations from 0-50 μM. The initial rates were determined by fitting a straight line to the linear portion of the progress curves (first 10 s after Ca^{2+} addition) (Figure S1). The resulting rate data were fitted to Michaelis-Menten curves for the visualization of enzyme inhibition. K_i, K_m, and V_{max} values for the reactions were obtained from simultaneously fitting the uninhibited and inhibited data to the full mixed enzyme inhibition equation below,

$$v = \frac{\frac{V_{max}}{1 + \frac{[I]}{K_{i2}}}[S]}{K_m \frac{1 + \frac{[I]}{K_{i1}}}{1 + \frac{[I]}{K_{i2}}} + [S]}$$

where K_{i1} is the dissociation constant for inhibitor from free enzyme, and K_{i2} is the dissociation constant for inhibitor from the ES complex.

For those inhibitors that appeared to follow competitive inhibition kinetics, the data was fit to the competitive inhibition equation below,

$$v = \frac{V_{max}[S]}{K_m\left(1 + \frac{[I]}{K_{i1}}\right) + [S]}$$

Simultaneous non-linear regression fitting was done by a similar method as Kakkar *et al.*[52] using the non-linear least squares fitting function of gnuplot.[53] All reactions were corrected for the inner filter effect as previously described[54] by measuring the fluorescence of increasing amounts

of substrate with a fixed concentration of free EDANS fluorophore and thereby calculating a correction factor.

Identifying the inhibitor binding site by photo-reactive cross-linking. Peptides were synthesized using the thioester deacylation methodology to establish a thiol group on the peptide for downstream conjugation.[55] The reactions proceeded by first exposing the peptides to cyclization conditions and then ring-opening with a thioacid. DTT and K_2CO_3 were used for deacylation of the resulting thioester. The thiol-containing peptide was conjugated to benzophenone-4-maleimide in DMF, deprotected under acidic conditions, and purified by reversed-phase flash chromatography. For more details, see Supporting Information. A control inhibition study was performed to ensure the photoreactive probes remained active. The photo-reactive probes were cross-linked to calpain using similar methods to those of O'Neil, *et al.*[56,57] Benzophenone-containing compounds am*[PGLo] and c*[PGALK] were each incubated with calpain at 5 and 10 molar excess (25 and 50 μM, respectively). A control reaction was carried out with equivalent amounts of DMSO. Inactive C105S mutant calpain-2 was present at 0.5 mg/mL (5 μM). The reaction took place in a solution of 10 mM HEPES pH 7.4, 10 mM DTT, and 4 mM $CaCl_2$, placed in 96-well Corning polystyrene plates, and allowed to proceed under long-wave UV light for 2.5 h. The photo-adduct products were then submitted to the Protein Function Discovery Facility at Queen's University for tryptic digestion and MALDI-TOF mass fingerprinting (see Supporting Information).

Results and Discussion

Peptide macrocyclization results in the formation of calpastatin-like β-turns

Building on the initial work of peptide macrocyclization with aziridine aldehyde dimers,[58] we recently observed a propensity for the cyclic products to form β-turns.[39] In the cyclization process, three additional atoms are introduced into the peptide backbone. This cyclization linker is comprised of an exocyclic amide and an aziridine moiety, the latter of which can react with a nucleophile (Figure 3A). The presence of the carbonyl group in close proximity to the peptide backbone allows the peptide to adopt a multitude of conformations with transannular hydrogen bonds. Peptide backbones of pentamers cyclized with the aziridine aldehyde methodology have been found to adopt β-turn structures in both solution phase (NMR) and solid phase (X-ray).[39] In the solid phase structure of c*[PGLGF], a type II β-turn centered on the Gly-Leu residues was observed, while in the solution phase, the turn was indexed by one residue, such that the turn was centered on the Pro-Gly residues and a type I β-turn was formed (Figure 3B).

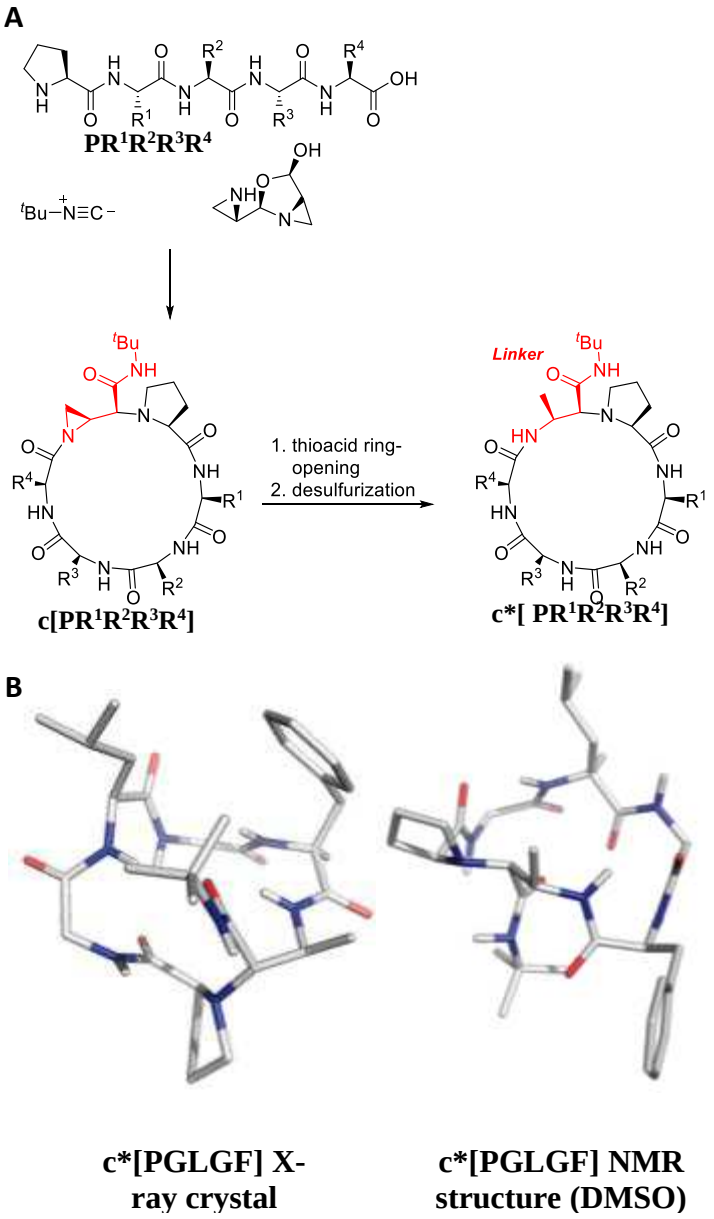

Figure 3. Macrocyclization of peptides to mimic natural calpastatin β-turn motifs. (**A**) Aziridine aldehyde-based macrocyclization provides access to β-turn motifs in peptides. The macrocycles are denoted with c*[$PR^1R^2R^3R^4$], where $PR^1R^2R^3R^4$ corresponds to the linear peptide pentamer precursor. Amino acids of the linear peptide precursor are shown in black, while the ring closure-associated chemical groups are highlighted in red. (**B**) Cyclic peptide c*[PGLGF], derived from linear peptide PGLGF, arranges into a distinct β-turn when observed

by X-ray in the solid state versus the solution phase structure in DMSO. c*[PGLGF] is shown in stick representation with oxygen atoms coloured red and nitrogen atoms coloured blue.

Aziridine aldehyde-mediated peptide cyclization was performed at 0.05 – 0.2 M concentration without appreciable amounts of cyclodimerization and polymerization by-products formed, which is a distinct improvement over conventional peptide cyclization methods.[55] A competing intramolecular reaction pathway led to peptidomimetics bearing an amidine functionality (Figure 4).[59] The amidine products are a novel structural class bearing a cycle-tail motif with a piperazinone-like core and linear peptide chain. The cyclization reaction favours cyclic peptide (Figure 3) products when pentamers formed from all L-amino acids are cyclized, and forms the amidine products predominantly with smaller linear peptides substrates or pentamers with varied side chain stereochemistry. Armed with the methodology to make two types of peptidic structures, β-turns with cyclic peptides and cycle-tail motifs with the amidine peptidomimetics, we turned to the crystal structures of calpastatin-inhibited Ca^{2+}-activated full-length calpain as a model for inhibitor development.

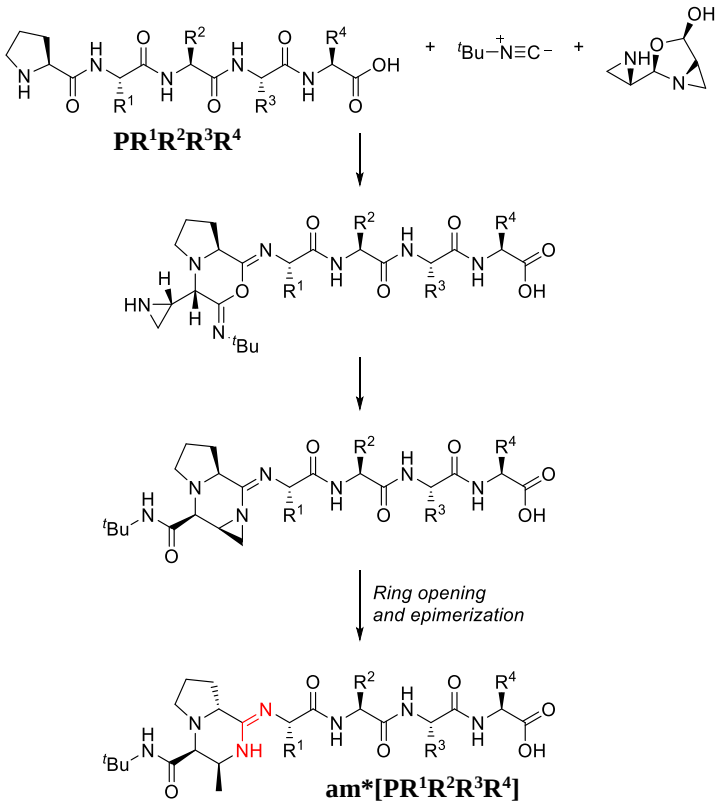

Figure 4. Cycle-tail motif peptides derived from aziridine aldehydes and isocyanide. The amidine (functionality highlighted in red) peptidomimetics are denoted with am*[$PR^1R^2R^3R^4$], where $PR^1R^2R^3R^4$ corresponds to the linear peptide pentamer precursor.

Modelling potential inhibitors on the β-turn structure of calpastatin in the calpain active site cleft.

Previously published methods for making cyclic peptides[39,58] provided an option for the design and modelling of peptides to mimic the conformation of calpastatin in the calpain active

site (Figure 5). Some of these initial models were analyzed using the molecular dynamics software package GROMACS.[41] These models were then used in docking simulations. MD simulations of calpain-2, taken from the calpastatin-bound calpain-2 structure, were used as representative structures to dock cyclic peptides using AutoDock4[46] and Glide[47-49]. The lowest energy conformations for the docked molecules clustered in the unprimed side of the active site cleft and involved interactions with the C2-like domain of calpain (Figure 5).

The tendency for our initial cyclic peptide designs to also interact with the C2L domain (green region in Fig. 5) in docking and MD experiments suggested that the synthesized peptides could potentially be specific inhibitors of calpain, because this domain is absent from other cysteine proteases.

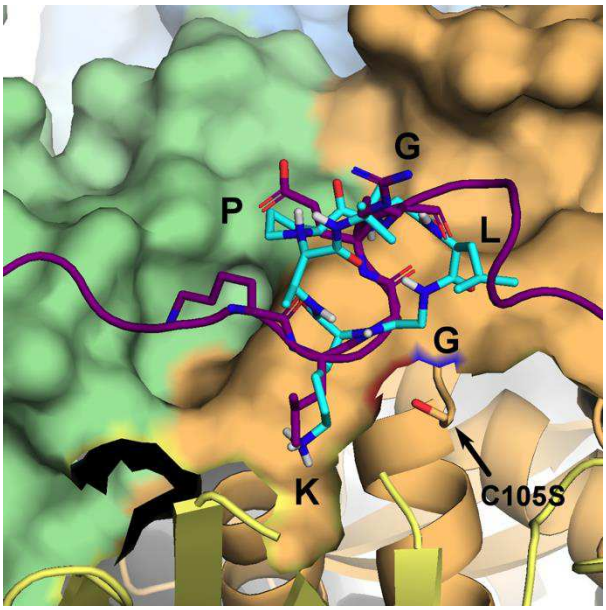

Figure 5. Mimicking the active site of calpastatin-bound calpain-2 with cyclic peptides. Close-up view of the calpastatin-bound calpain-2 active site. A representative cyclic peptide docking result from Glide is shown for c*[PGLGK] (cyan), with polar hydrogens displayed and residues labelled, while calpastatin is shown in purple. N and O atoms are coloured blue and red,

respectively. The structure is shown with a partial cut-away to give a clear view of the bound inhibitors. Domain colours (C2L – green, PC2 – orange, PC1 – yellow) are as shown in Fig.1.

Macrocyclic and cycle-tail motif peptidomimetic library

All peptides were made with Pro at the *N*-terminus to ensure efficient cyclization. Based on previous work with tetramers and pentamers containing two D-amino acids, which tended to undergo amidine formation, we split the library design into two groups. The first group, made of cyclized pentamers (Figure 3A), was aimed at mimicking the inhibitory calpastatin β-turn sequence at KLG. At the Lys, the side chain length requirement was investigated using the increasingly shorter amine-bearing side chain residues Orn, Dab, and Dap. Based on the crystal structure of c*[PGLGF], which positioned the β-turn around Gly-Leu, the basic residues were placed in the fifth position. Finally, as it was previously seen that the solution phase structure of c*[PGLGF] could index the turn by one residue and form the β-turn around Pro-Gly (Figure 3B), basic residues were also placed in the third position.

Cycle-tail motif peptidomimetics comprised the second group of peptides formed from the multicomponent reaction of aziridine aldehyde dimers, peptides, and isocyanides (Figure 4). This set of inhibitor probes was also designed to screen permutations of KLG tripeptide sequence and length of amine-bearing side chains. As the binding mode was less certain, the order of the KLG tripeptide was also perturbed in a subset of the peptidomimetic probes. We anticipated that our compounds would inhibit calpain with radically different properties from Abell's tripeptide

peptidomimetics (Figure 2), which relied on covalent binding to inhibit with high IC_{50}s and were not selective against cathepsins.[24]

Screening of peptide library using fluorescence-based protease assays

When the cyclized pentamers and peptidomimetics were screened using a fluorescence-based enzyme activity assay against calpain-2, macrocyclic compounds demonstrated significant levels of inhibition of calpain-2 (Figure 6A). Approximately 60% of the macrocyclic compounds showed levels of inhibition of calpain-2 that were ≥ 25% at concentrations of 100 μM. Two macrocyclic peptides, c*[PGALK] and c*[PGSGO], showed reproducibly high levels of inhibition of calpain-2 (> 85%) at this concentration.

Levels of inhibition by the peptidomimetic set of compounds were similar to those of the macrocyclic forms with approximately half of the cycle-tail motif peptidomimetics showing ≥ 25% inhibition at concentrations of 100 μM. One peptidomimetic, am*[PLKG], also showed reproducibly high levels of inhibition of calpain-2 (> 85%) at the 100 μM concentration, while another, am*[PGLo], similarly showed high levels of inhibition of calpain-2 at concentrations of 100 μM, but with more variation (from 16-72%) (Figure 6B).

Full-length calpain enzyme has been found to undergo extensive autoproteolysis *in vitro* upon activation[60]. The autoproteolysis of calpain was examined in the context of these experiments to ensure apparent inhibition of calpain was not due to loss of activity enzyme. Under the experimental conditions used and the short time frame analyzed for activity, autoproteolysis was not found to be a significant source of inactivation of calpain-2 (see SI).

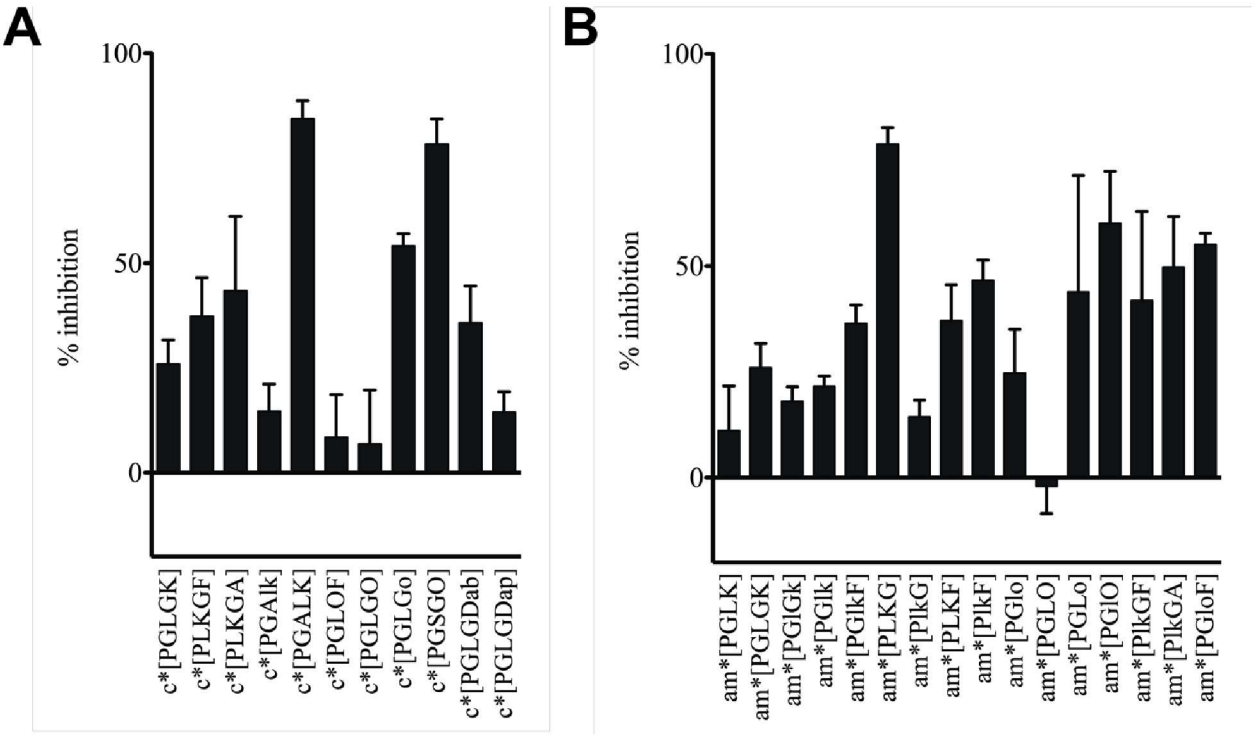

Figure 6. Inhibition screening of peptide compounds. (**A**) Hydrolysis of fluorescent substrate by calpain 2 in the presence of cyclic peptides, and (**B**) cycle tail motif peptidomimetics. All compounds were screened at 100 μM. Error bars represent the standard deviation resulting from triplicate assays. Inhibition was determined as a percentage of the initial reaction velocity for the control reaction containing equivalent amounts of DMSO. The amino acid ornithine, Orn, is represented by "O".

Protease specificity of initial peptide library hits

Calpains share many substrates and inhibitors with other cysteine proteases of their clan, due to structural and mechanistic similarities in their active site region. This is illustrated in the example where the active site cleft region of calpain 2 has been overlaid on cathepsin L, a

physiologically relevant papain like enzyme (Figure 7). Cathepsin L protease was aligned by backbone carbon atoms to calpain 2 residues of the catalytic triad and adjoining regions (calpain 2 residues 105 114, 252 268, and 286 292). The alignment between the two proteases was close in these active site regions with an RMSD of 0.415 Å, signifying the grand challenge of achieving selectivity between these proteases. The absence of an equivalent region in cathepsin L to the calpain 2 C2L domain (labelled, green circle) on the unprimed side of the active site cleft, and the loop regions from residues 160 176 on the primed side of the active site cleft (labelled, orange circle) suggested that specificity could be possible with our inhibitors if they interacted with the C2L region.

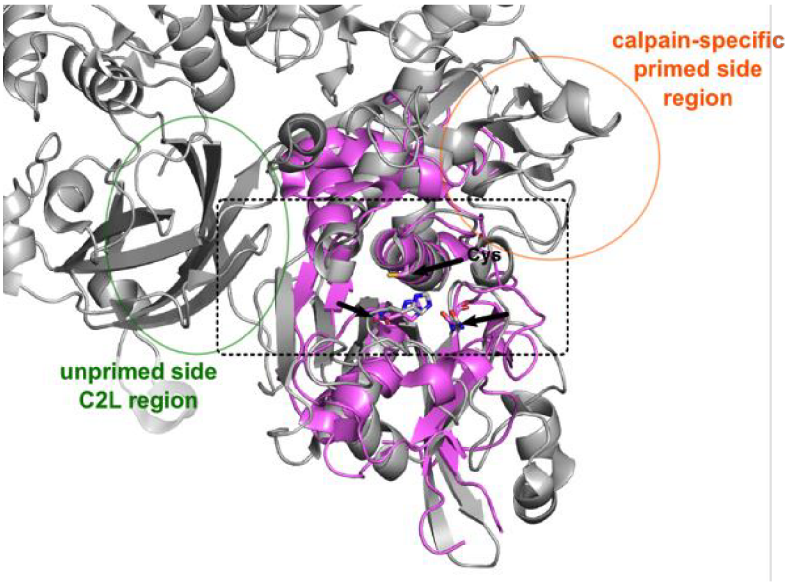

Figure 7. Comparison of the active site region of cathepsin L and calpain 2. The structures of Ca^{2+} activated rat calpain 2 (grey) (PDB: 3BOW),[15] and human cathepsin L (pink) (2YJ2)[61] are displayed in ribbon representation except for the catalytic triad residues in sticks, where N, O, and S atoms are coloured blue, red, and yellow, respectively. The general area of the active site cleft is highlighted by a dotted black box.

Due to the high structural similarities of cysteine proteases, it was necessary to test any potential inhibitors for protease selectivity. Inhibition assays using fluorogenic substrates were performed against calpain-1 protease core, papain, and cathepsin L (Figure 8). We observed potent but reduced inhibition of calpain-1. As the calpain-1 protease core construct lacks the auxiliary domains of calpain, it gave us the opportunity to deduce if our inhibitors exhibited their effect through the C2L domain. Indeed, we observed negligible inhibition of calpain-1 protease core, which meant that our study peptides interacted with more than just the PC1 and PC2 domains of the protease core. The negative inhibition seen of the calpain-1 protease core by these compounds indicates activation of the enzyme. Previous studies have suggested the inherent flexibility of the protease core, caused by a lack of ancillary domains, results in lower activity than the full-length calpain enzyme[13]. It is possible that the protease core domains could be stabilized upon binding to some compounds, and thus display increased protease activity. It should be noted that currently, the only recombinantly-expressing, active construct of the protease core domains is that of calpain-1.

c*[PGALK] and c*[PGSGO] showed some specificity for calpain-2 over calpain-1 (respectively, c*[PGALK]: ~ 84% and ~ 45%, c*[PGSGO]: ~ 78% and ~ 38%). It is uncertain why there could be differential inhibition between calpains with these macrocycles because of the high sequence and structural homology of calpains-1 and -2, especially in the active site cleft where the presumed competitive inhibitors would bind.

Papain and cathepsin L enzymes were used to investigate any differences based on similarities in structural characteristics of the catalytic triad. The four selected lead compounds, c*[PGALK], c*[PGSGO], am*[PLKG], and am*[PGLo], showed little to no inhibition of papain, but high levels of inhibition (> 85%) of cathepsin L.

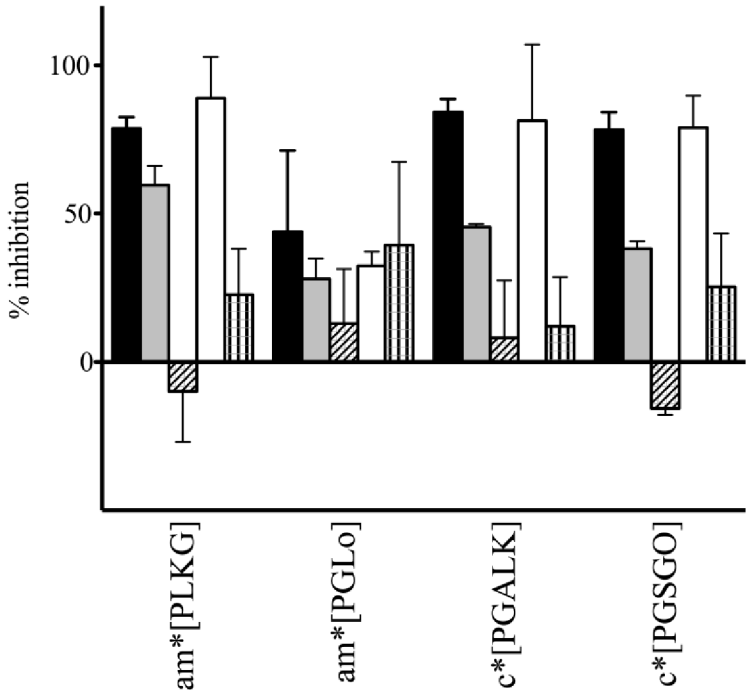

Figure 8. Protease specificity of lead compounds. The hydrolysis of fluorescent substrate by calpain 2 (black), calpain 1 (light grey), calpain 1 protease core (diagonal lines), cathepsin L (white), and papain (vertical lines) in the presence of each of the four selected calpain 2 inhibiting peptides. All compounds were screened at 100 μM. Error bars represent the standard deviation resulting from triplicate assays. Inhibition was determined as a percentage of the initial reaction velocity for the control reaction containing equivalent amounts of DMSO. The amino acid ornithine, Orn, is represented by "O".

In general, for both macrocycle and cycle tail motif peptidomimetics, the widely variable inhibition levels across proteases suggested a strong dependence on amino acid choice and positioning in the peptide substrates for their interactions with calpain. Tight protein ligand interactions depend on the structure of the peptide, whether cycle tail motif or macrocycle, and

the orientation in the binding site, both of which are directly affected by peptide sequence and the cyclization linker atoms. Moreover, the lack of protease core inhibition indicated that the inhibitors were interacting with other regions such as the C2L domain. However, low selectivity against cathepsin L implied that the inhibitors were not solely binding to the C2L domain. Finally, peptides but am*[PGLo], shared a common selectivity profile, which warranted a closer look by inhibitions kinetics.

Enzyme kinetics analyses and inhibition mechanisms.

To determine the mode of inhibition of the lead cyclic compounds with calpain-2, extensive analyses of enzyme kinetics were performed using the fluorogenic substrate assay. Using the four potent lead compounds, the initial rates of substrate cleavage by calpain-2 were fit to the Michaelis-Menten plot for uninhibited and inhibited reactions (Figure 9A-D).

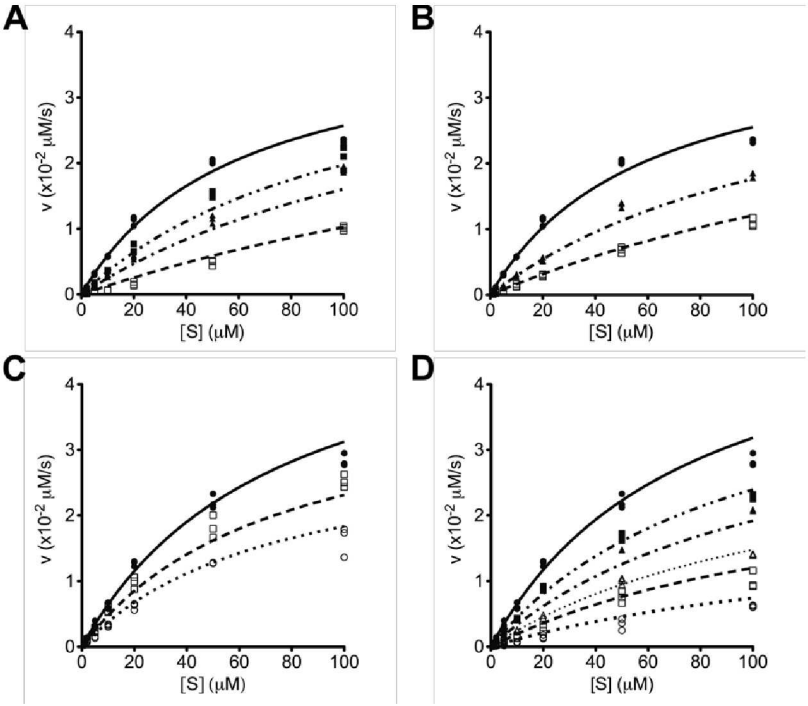

Figure 9. Michaelis Menten curves for the inhibition of calpain 2 by four lead compounds. The initial rates of (EDANS) EPLFAERK (DABCYL) substrate cleavage by calpain 2 in the absence and presence of each of (**A**) am*[PLKG], (**B**) c*[PGALK], (**C**) am*[PGLo], and (**D**) c*[PGSGO] were obtained and fit to the Michaelis Menten equation. Reactions were performed at 298 K in a reaction buffer consisting of 10 mM HEPES pH 7.4 and 10 mM DTT, and initiated by the addition of 10 mM $CaCl_2$. Data were obtained in triplicate at increasing concentrations of compound: 0 μM (solid line, ●), 10 μM (2 dot dashed line, ■), 20 μM (dot dashed line, ▲), 35 μM (small dotted line, △), 50 μM (dashed line, □), and 100 μM (dotted line, ○).

To accurately obtain reaction parameters, the initial rate of substrate cleavage by calpain 2 was simultaneously fit to the full mixed enzyme inhibition equation for uninhibited and inhibited reactions. This allowed for the calculation of the inhibition constants, K_{i1} and K_{i2}, as well as K_m and V_{max} (Table 1). Within the experimental error of fitting data to the equations and

parameters, it was determined that of the four lead compounds, am*[PGLo] functioned as a non-competitive inhibitor, am*[PLKG] and c*[PGALK] showed competitive inhibition, and c*[PGSGO] fit the mixed inhibitor category when tested with calpain-2. The compounds that were found to be competitive inhibitors showed higher standard error of the parameters when fit to the mixed inhibition equation. Thus, these data were refit to the competitive inhibition equation and their parameters reported. The B27 WT peptide inhibitor based on calpastatin was used as a control to ensure accurate data analyses, and showed competitive inhibition of approximately 16.8 ± 1.7 nM, close to the previously reported value of 8.7 ± 2 nM.[61]

Table 1: Summary of inhibition kinetics after fitting data to the full mixed enzyme inhibition equation.

Compound	K_{i1} (μM)	K_{i2} (μM)	Inhibition model
B27 WT peptide	$16.8 \times 10^{-3} \pm 1.7 \times 10^{-3}$ [a]	n/a	competitive
am*[PLKG]	12.2 ± 0.8 [a]	n/a	competitive
c*[PGALK]	16.6 ± 1.0 [a]	n/a	competitive
c*[PGSGO]	20.3 ± 2.0	45.6 ± 19.8	mixed
am*[PGLo]	153.7 ± 27.6	119.4 ± 37.9	non-competitive

Calpain-2 cleavage of the fluorescent substrate (EDANS)-EPLFAERK-(DABCYL) was monitored over time. Inhibition kinetics were obtained by fitting initial rate data to the full mixed enzyme inhibition equation. Reactions were performed at 298 K in a reaction buffer consisting of 10 mM HEPES pH 7.4 and 10 mM DTT. Calpain activity was initiated through the addition of 10 mM $CaCl_2$. n/a denotes compounds whose fit of data to the full mixed equation resulted in an extremely large K_{i2} value with unreasonably high margin of error, and therefore exhibited competitive inhibition. [a] Compounds were found to be competitive inhibitors and showed lower standard error for

parameters when fit to the competitive inhibition equation than when fit to the mixed inhibition equation. Their parameters are thus reported according to the fit to the competitive equation.

While our initial efforts were to design competitive macrocyclic peptide inhibitors with specificity for calpain through interactions with the C2L domain, only two of the four most potent compounds exhibited competitive inhibition. The other two showed non-competitive inhibition and mixed mode inhibition. Ideally, the macrocycle conformation could help form a calpastatin-like β-turn, while the residues Leu and Lys, responsible for a key interaction between calpastatin and calpain, could anchor the macrocycles in the intended binding site. It is apparent that macrocyclic compounds without these crucial residues might then result in mixed inhibition, as is the case with c*[PGSGO], a non-competitive inhibitor. Further studies may help elucidate the role that ring size and flexibility may play in terms of inhibition potency. The cycle-tail motif peptidomimetics display a novel peptide structure for calpain inhibition, yet there is seemingly little information to be gathered as to a pattern for preferred residues (Figure 6B). It is possible that, as is the case for c*[PGSGO], the peptide sequence can change the binding site of the peptide and thus the mode of inhibition as well. Investigating these cycle-tail motif peptidomimetics compounds further by structural studies will be crucial to defining the new binding pockets and structure-activity relationships.

The most potent of all analyzed study compounds was the competitively-inhibiting am*[PLKG] with a K_i of 12.2 ± 0.8 μM. K_i values were calculated rather than IC_{50} values in order to assess affinity for the enzyme as well as to determine the inhibition mechanism. The level of inhibition seen with am*[PLKG] approaches the range of potency found with other covalent and non-covalent peptidomimetic competitive inhibitors of calpain.[26] Specifically, when comparing these levels of inhibition to other inhibitors designed based on the calpain-calpastatin

structure, we see that am*[PLKG], despite lacking covalent attachment to the enzyme, inhibits calpain with equal potency as the irreversibly-binding α-helical inhibitory peptide 3c (K_i of 10.2 ± 2.9 μM).[62] Most calpain inhibition studies report IC_{50} values instead of K_i values. The former are easier to compute but are less rigorous than the latter. Although it is difficult to equate one to the other, as the relationship between IC_{50} and K_i depends on inhibition mechanism as well as reaction conditions,[63,64] the larger macrocyclic inhibitors of calpain reported previously are within the same order of magnitude as am*[PLKG],[24] and show some selectivity for calpain. Interestingly, am*[PLKG] as the most potent compound in this series retained the conserved residues of the calpastatin β-turn structure, albeit in mixed order. It remains to be seen from an enzyme-inhibitor complex structure if this is the reason for the potency for cycle-tail motif peptidomimetics.

Molecular docking of c[PGALK] NMR structures to calpain-2.*

Because the macrocyclic peptide c*[PGALK] was found to competitively inhibit calpain-2, we modelled its inhibition by docking studies. c*[PGALK] was modelled first with Macromodel (simulated annealing and Monte Carlo multiple minimum (MCMM) with the OPLS-2005 force field) and we considered the 30 lowest energy structures that fit the NMR data. To accurately sample interaction of the side chains with the protein while accounting for the hydrogen bonding network across the cycle backbone itself, all 30 lowest energy structures were docked individually with torsional constraints on the backbone and peptide bonds while keeping the side chains flexible. AutoDock4 and Glide provided the same structures as the most favourable poses. Analysis of the representative top poses from Glide, ranked by lowest free

energy of binding, showed deep binding within the unprimed site (Figure 10). The agreement between two different docking programs and protocols gave support to the binding of c*[PGALK] at the unprimed side of the active site cleft, consistent with the experimentally observed competitive inhibition. The vast majority of top poses from both computational suites were slight variations of this structure, either by a slight tilt in the central macrocycle or by slight movement of the side chains, but remained nonetheless very similar. Many key contacts were formed between c*[PGALK] and the calpain 2 structures, including two hydrogen bonds to the peptide backbone as well as three hydrogen bonds to the protonated Lys side chain (Figure 10). The *t* butyl group from the backbone ring closure lies in a hydrophobic pocket created by the C2L and PC2 domains.

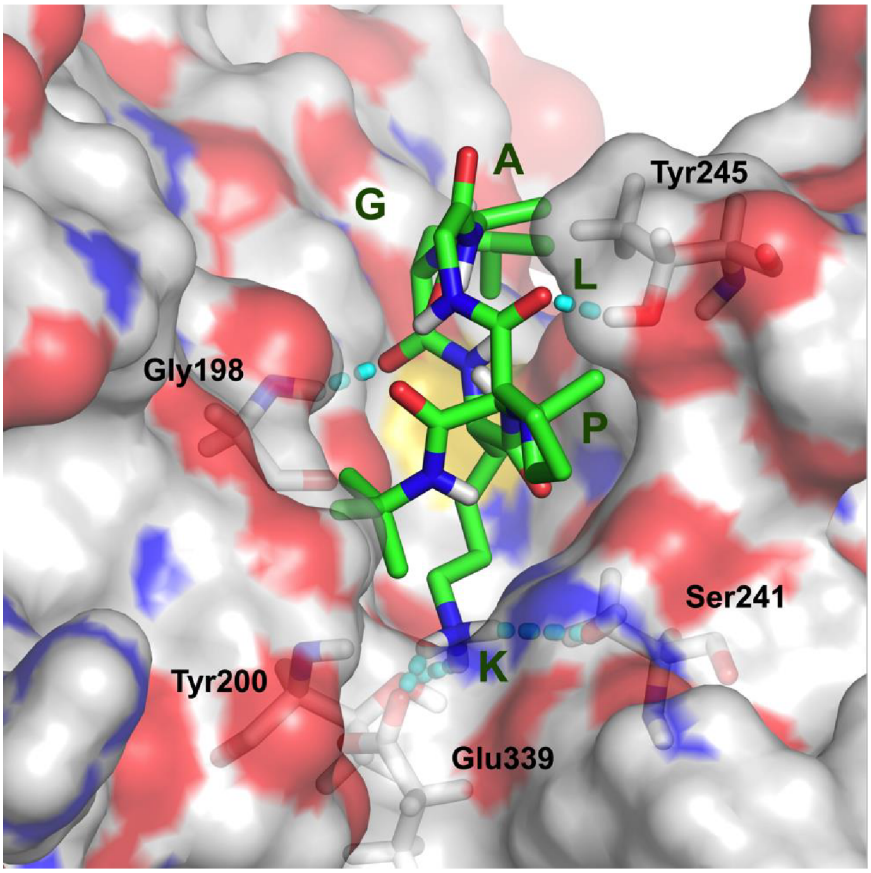

Figure 10. Lowest binding energy docking pose of c*[PGALK] to calpain-2. The top docking pose from Glide, classified from the calculated free energy of binding by Prime MM-GB/SA, of c*[PGALK] (residues labelled) bound to Ca^{2+}-activated calpain-2 (originating from PDB: 3BOW) seen along the active site cleft from the unprimed side. Calpain-2 is shown in surface representation with residues key for hydrogen bonding to the inhibitor in stick format and labelled. Hydrogen bonding contacts are labeled with cyan dashes. N and O atoms of both calpain-2 and the peptidomimetic are coloured blue and red, respectively.

Docking results using c*[PGALK] conformers with NMR considerations were more reliable than those of peptides starting from unbiased conformational sampling, lending more credence to the newly docked conformation of c*[PGALK]. Thus, the determination of NMR solution structures for more compounds may help to obtain more plausible docking results in the future. Further modifications to residues pointing toward pockets on the C2L domain, including modifications to the cyclization linker *t*-butyl group, may increase the number and quality of interactions, and increase inhibition potency and specificity. This would allow for further assessment of the docking procedure and validation of docking results.

Improvement of potency and selectivity of the peptidomimetic am[PGLo]*.

True non-competitive inhibitors of calpains have been scarce, but are highly desired due to the potential for designing increasingly calpain-specific inhibitors by accessing an allosteric site. As a second-generation of peptidomimetic compounds, modifications were made to the non-competitive inhibitor am*[PGLo], varying both the Leu and D-Orn residues, to investigate

potential improvements in both potency and specificity for calpain-2 over other similar cysteine proteases. Through initial screening of calpain-2, calpain-1, cathepsin L, and papain, using the fluorogenic substrates for each enzyme, four compounds were found to increase both potency and specificity of inhibition of calpain-2: am*[PGIo], am*[PGVo], am*[PGL-D-Dab], and am*[PGLq] (Figure 11). The four compounds showed significantly higher inhibition of calpain-2 over cathepsin L. For example, am*[PGVo] was almost twice as inhibitory against calpain-2 as am*[PGLo] (79% vs 44% inhibition, respectively) while showing half the inhibition of am*[PGLo] against cathepsin L (17% vs 32%, respectively). As discussed previously, any negative inhibition seen suggests activation of the enzyme possibly through structural stabilization of the active conformation. Further studies would be needed to characterize this activation. Attempts were made to further improve inhibition by combining the sequences of am*[PGIo] and am*[PGVo] with am*[PGL-D-Dab] to form am*[PGV-D-Dab] and am*[PGI-D-Dab]. Inhibition increased for calpain-1; however, there was essentially no change with respect to calpain-2 inhibition levels. The improvements can likely be attributed to a preference for branched hydrophobic residues at the third position in the peptidomimetic compounds and size-specific charged residues at the fourth position, although this does not explain the plateau of inhibition seen for the merged sequences. Additional protein structural work will elucidate the binding characteristics of cycle-tail motif peptidomimetics to calpain.

The four improved second-generation compounds displayed, in some cases, specificity for calpain-2 over calpain-1. At 100 μM, am*[PGIo] inhibited calpain-2 to ~ 67% but failed to inhibit calpain-1 in a significant way (~ 14%). It is possible that branched hydrophobic residues at R^3 are responsible for interaction in a small neighbouring pocket against calpain-2 that may be smaller on the surface of calpain-1. This would be consistent with the ability of the small side

chain Ala variant am*[PGAo] to inhibit calpain 2 and calpain 1 equally well (~ 66% and ~54%, respectively), and the reduced inhibition by the bulkier variant am*[PGFo] (~ 39% and ~ 28%, respectively). Further studies are needed in order to confirm the mode of inhibition for these second generation compounds. However, it is feasible for non competitive and mixed inhibitors, specifically am*[PGLo] and c*[PGSGO], to bind to small patches on calpain that vary slightly between calpain 2 and calpain 1, although the mechanism behind allosteric inhibition of calpains and the possibility for truly isoform specific inhibitors remain unknown.

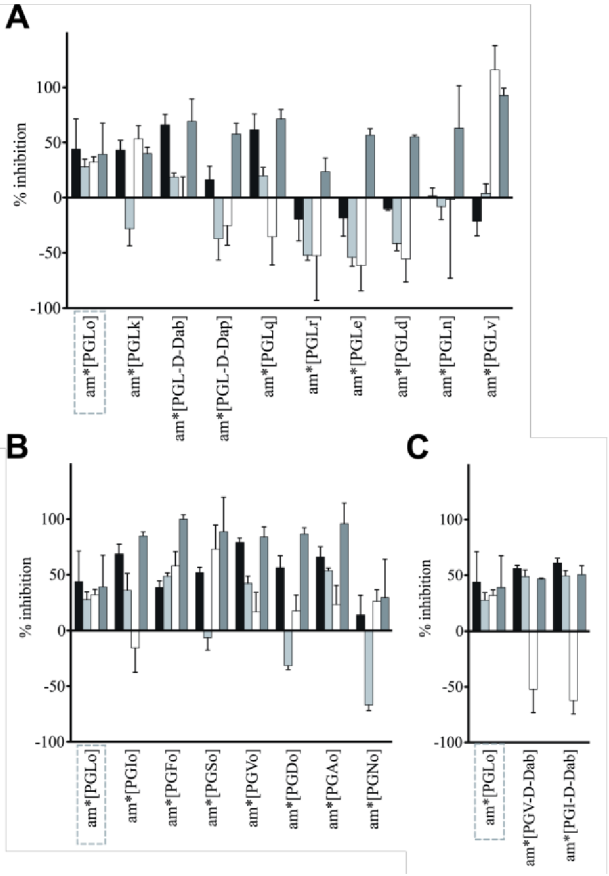

Figure 11. Inhibition of cysteine proteases by variants of am*[PGLo]. The hydrolysis of fluorescent substrate by calpain 2 (black), calpain 1 (light grey), cathepsin L (white), and papain (dark grey) in the presence of second generation calpain 2 peptidomimetic inhibitors. The

original sequence am*[PGLo] was varied at (**A**) D-Orn, (**B**) Leu, and (**C**) both D-Orn and Leu. Highlighted with a grey dotted box is the original compound am*[PGLo] in all three graphs. All compounds were screened at 100 μM. Error bars represent the standard deviation resulting from triplicate assays. Inhibition was determined as a percentage of the initial reaction velocity for the control reaction containing equivalent amounts of DMSO.

Identification of peptide binding sites and a novel allosteric inhibition site.

With am*[PGLo] identified as a non-competitive inhibitor of calpain, it was necessary to further characterize the binding site. We were not able to generate co-crystals of calpain with am*[PGLo] and thus turned to identifying the binding site by covalent modification of calpain-2 and protein sequencing (see Supporting Information). Similarly, photo-reactive c*[PGALK] was synthesized to act as a control since it was shown to inhibit calpain competitively. If it was seen to label residues in proximity to the active site of calpain, then this would confirm the validity of the method. In a control experiment, both of the photo-reactive compounds inhibited calpain-2 to the same extent as the original compounds lacking the photo-reactive moiety (Figure S2).

Photo-am*[PGLo] and photo-c*[PGALK] were covalently attached by exposure to UV light to the inactive C105S mutant calpain-2 in the presence of calcium. Following tryptic digest, fragment masses were compared between photo-reactive compound conditions and the DMSO control to identify calpain sequences with photo-adducts. The sequences with a mass difference equal to the photo-reactive compound are shown in Supporting Information. These sequences were mapped to the calpain-2 structure (Figure 12). While the bound fragments may appear

disperse, in actuality one fragment is visible from multiple angles. For example, the tryptic fragment identified as residues 338-357 can be seen on both sides of the enzyme (Figure 11B). At both 25 and 50 μM compound concentrations, aiming to limit side reactions and maintain consistent methodology, there was no difference in identified sequences, for either am*[PGLo] or c*[PGALK], likely due to the high molar excess of compound over enzyme and suggests a lack of additional unselective binding.

The crosslinking data showed that c*[PGALK] bound calpain-2 through interactions with the C2L domain on the unprimed side of the active site cleft, at around the P3 and P4 subsites (Figure 12). Furthermore, the binding site location of c*[PGALK] was consistent with experimental inhibition data displaying competitive inhibition, *in silico* docking models, and protease selectivity experiments, thereby lending credibility to this method.

For the non-competitive inhibitor am*[PGLo], the crosslinking data showed covalent labelling of calpain-2 at a new binding site (Figure 12). The novel allosteric site was located at the center region, common to all calpain domains. This site can be described as at the interface between the C2L domain and the PC1 and PC2 domains, on the opposite side of the enzyme from the active site cleft. Binding at this location by am*[PGLo] could inhibit calpain-2 by interfering with dynamics of the protease core domains, or indeed the entire enzyme, during hydrolysis of substrate.[65,66] Another potential mechanism for allosteric inhibition at this location could be that by disturbing the tight interactions between the protease core domains and the C2L domain, the protease core domains would no longer be stabilized, resulting in lower overall activity of the enzyme.[13]

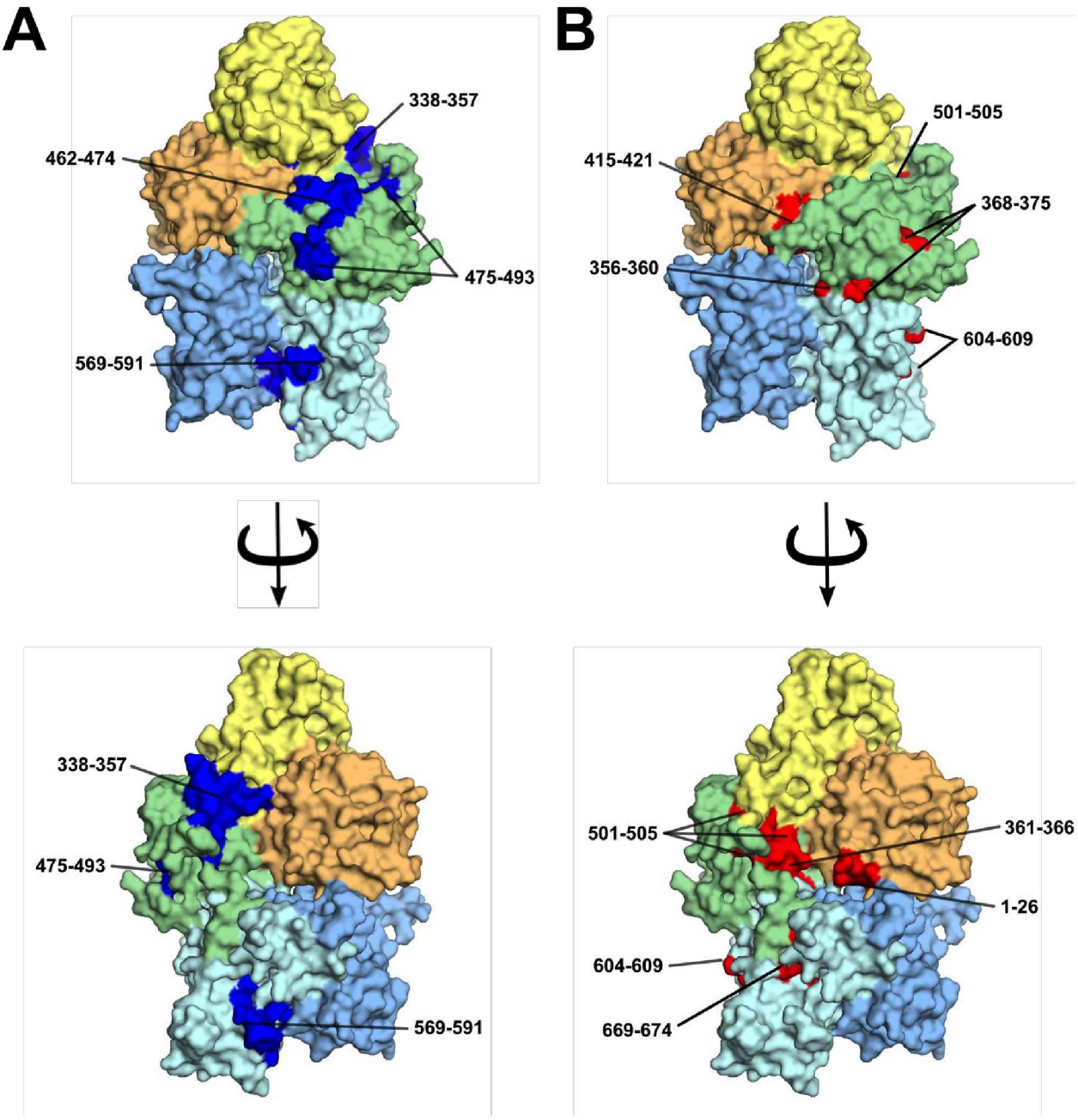

Figure 12. Binding sites of c*[PGALK] and am*[PGLo] on calpain 2. The inhibitor binding locations identified by photo reactive adducts and subsequent tryptic digest are shown mapped onto the structure of calcium bound calpain 2, shown as surface representation with domains

coloured as in Figure 1 (PDB: 3BOW). The tryptic digest fragments found to bind (**A**) c*[PGALK] (bright blue) and (**B**) am*[PGLo] (bright red) are shown, and labelled by residue numbers.

Both c*[PGALK] and am*[PGLo] seem to also bind to locations in the hydrophobic clefts of the PEF domains (light cyan, Figure 12). These locations are likely due to non-specific binding at excess concentrations of compounds, as previous work has shown the PEF domains to be unlikely domain targets for inhibition of calpains.[67]

The data from these photo-reactive binding assays can serve as a starting point for improvement and rationalizing the structure-activity relationship of both am*[PGLo] and c*[PGALK], as well as the other variants. Structural data from X-ray crystallographic methods would pinpoint the exact residues necessary for inhibition by these compounds and may, ultimately, be necessary for improving inhibition potency and selectivity.

Conclusion

Potent, calpain-specific inhibitors are sought as tools for studying the physiological roles and substrates of calpain, and as treatments for such conditions as traumatic brain injury, Alzheimer's disease, heart attack, and stroke. The advent of calpastatin-bound calpain structures has allowed for the synthesis of calpain-specific inhibitors based on structural features of the calpain-calpastatin complex. Medium-sized cyclic peptides demonstrated the ability to function

as protease inhibitors against calpain, papain, and cathepsin L, as did the cycle-tail motif peptidomimetics based on the same calpastatin-like variations of the KLGE sequence.

Four main lead compounds, c*[PGALK], c*[PGSGO], am*[PLKG], and am*[PGLo], displayed competitive, non-competitive, or mixed inhibition of calpain with K_i values in the mid- to low-μM range, which are comparable to those of other calpain peptidomimetic inhibitors reported in literature. Two of the compounds, the competitively inhibiting c*[PGALK] and am*[PLKG], showed specificity for calpain over cathepsin L. Sequence variations of the am*[PGLo] sequence improved the non-competitive inhibition, and greatly increased specificity for calpain over cathepsin L. Photo-reactive versions of the compounds c*[PGALK] and am*[PGLo] were successfully employed to locate their binding sites. The binding of am*[PGLo] to the central, unexplored region of calpain-2 demonstrated the potential discovery of a calpain allosteric site, and offers an explanation to the inhibitory nature of the cycle-tail motif peptidomimetics. In addition, the improvement of potency and selectivity for sequence variations of am*[PGLo] could be due to tighter interactions with residues unique to the C2L domain of calpain. Future goals are to further improve both potency and specificity of these peptide inhibitors and to structurally determine their binding sites on calpain.

Acknowledgements

We thank Sherry Gauthier for technical assistance. This work was funded by CIHR/NSERC-CHRP- project # CPG-112350. KL is the recipient of a Queen's University R.J. Wilson Graduate Fellowship, PLD holds the Canada Research Chair in Protein Engineering.

We thank the Natural Sciences and Engineering Research Council of Canada, CQDM - Québec Consortium for Drug Discovery, Ontario Genomics Institute, and Ontario Graduate Scholarship Program (S.Z.) for financial support.

The authors wish to acknowledge the Canadian Foundation for Innovation, project number 19119, and the Ontario Research Fund for funding of the Centre for Spectroscopic Investigation of Complex Organic Molecules and Polymers.

Supporting Information Availability

Supporting information available: Synthesis and characterization data for study compounds; enzyme inhibition kinetics; data and procedure for photo-reactive labelling of calpain

Author Information

Corresponding Author

*Peter Davies: peter.davies@queensu.ca; 613-533-2983

*Andrei K. Yudin: ayudin@chem.utoronto.ca; 416 946 5042

*Serge Zaretsky: serge_zaretsky@msn.com; 908-502-8552

Abbreviations

AMC 7-amino-4-methylcoumarin

C2L C2-like

DABCYL 4-((4-(dimethylamino)phenyl)azo)benzoic acid

EDANS 5-((2-aminoethyl)amino)naphthalene-1-sulfonic acid

MCMM Monte Carlo multiple minimum

MM-GB/SA molecular mechanics with generalised Born and surface area solvation

PC protease core

PEF penta-EF hand

TFE trifluoroethanol

References

(1) Ono, Y.; Sorimachi, H. Calpains - An Elaborate Proteolytic System. *BBA - Proteins Proteom.* **2012**, *1824* (1), 224–236.

(2) Wendt, A.; Thompson, V. F.; Goll, D. E. Interaction of Calpastatin with Calpain: A Review. *Biol. Chem. 385* (6), 465-472.

(3) Goll, D. E.; Thompson, V. F.; Li, H.; Wei, W.; Cong, J. The Calpain System. *Physiol. Rev.* **2003**, *83* (3), 731–801.

(4) Bertipaglia, I.; Carafoli, E. Calpains and Human Disease. In *Calcium Signalling and Disease*; Subcellular Biochemistry; Springer Netherlands: Dordrecht, 2007; Vol. 45, pp 29–53.

(5) Carragher, N. Calpain Inhibition: A Therapeutic Strategy Targeting Multiple Disease States. *Curr. Pharm. Des.* **2006**, *12* (5), 615–638.

(6) Raynaud, F.; Marcilhac, A. Implication of Calpain in Neuronal Apoptosis. *FEBS J.*

2006, *273* (15), 3437–3443.

(7) Richard, I.; Broux, O.; Allamand, V.; Fougerousse, F.; Chiannilkulchai, N.; Bourg, N.; Brenguier, L.; Devaud, C.; Pasturaud, P.; Roudaut, C.; Hillaire, D.; Passos-Bueno, M.-R.; Zatz, M.; Tischfield, J. A.; Fardeau, M.; Jackson, C. E.; Cohen, D.; Beckmann, J. S. Mutations in the Proteolytic Enzyme Calpain 3 Cause Limb-Girdle Muscular Dystrophy Type 2A. *Cell* **1995**, *81* (1), 27–40.

(8) Vosler, P. S.; Brennan, C. S.; Chen, J. Calpain-Mediated Signaling Mechanisms in Neuronal Injury and Neurodegeneration. *Mol. Neurobiol.* **2008**, *38* (1), 78–100.

(9) Maly, D. J.; Huang, L.; Ellman, J. A. Combinatorial Strategies for Targeting Protein Families: Application to the Proteases. *Chembiochem* **2002**, *3* (1), 16–37.

(10) Croall, D. E.; Ersfeld, K. The Calpains: Modular Designs and Functional Diversity. *Genome Biol.* **2007**, *8* (6), 218.

(11) Pietsch, M.; Chua, K. C. H.; Abell, A. D. Calpains: Attractive Targets for the Development of Synthetic Inhibitors. *Curr. Top. Med. Chem.* **2010**, *10* (3), 270–293.

(12) Sorimachi, H.; Hata, S.; Ono, Y. Impact of Genetic Insights Into Calpain Biology. *J. Biochemistry* **2011**, *150* (1), 23–37.

(13) Campbell, R. L.; Davies, P. L. Structure–Function Relationships in Calpains. *Biochem. J.* **2012**, *447* (3), 335–351.

(14) Moldoveanu, T.; Hosfield, C. M.; Lim, D.; Elce, J. S.; Jia, Z.; Davies, P. L. A Ca2+ Switch Aligns the Active Site of Calpain. *Cell* **2002**, *108* (5), 649–660.

(15) Hanna, R. A.; Campbell, R. L.; Davies, P. L. Calcium-Bound Structure of Calpain and Its Mechanism of Inhibition by Calpastatin. *Nature* **2008**, *456* (7220), 409–412.

(16) Moldoveanu, T.; Campbell, R. L.; Cuerrier, D.; Davies, P. L. Crystal Structures of

Calpain–E64 and –Leupeptin Inhibitor Complexes Reveal Mobile Loops Gating the Active Site. *J. Mol. Biol.* **2004**, *343* (5), 1313–1326.

(17) Moldoveanu, T.; Gehring, K.; Green, D. R. Concerted Multi-Pronged Attack by Calpastatin to Occlude the Catalytic Cleft of Heterodimeric Calpains. *Nature* **2008**, *456* (7220), 404–408.

(18) Cuerrier, D.; Moldoveanu, T.; Inoue, J.; Davies, P. L.; Campbell, R. L. Calpain Inhibition by A-Ketoamide and Cyclic Hemiacetal Inhibitors Revealed by X-Ray Crystallography. *Biochemistry* **2006**, *45* (24), 7446–7452.

(19) Li, Q.; Hanzlik, R. P.; Weaver, R. F.; Schönbrunn, E. Molecular Mode of Action of a Covalently Inhibiting Peptidomimetic on the Human Calpain Protease Core. *Biochemistry* **2006**, *45* (3), 701–708.

(20) Qian, J.; Cuerrier, D.; Davies, P. L.; Li, Z.; Powers, J. C.; Campbell, R. L. Cocrystal Structures of Primed Side-Extending A-Ketoamide Inhibitors Reveal Novel Calpain-Inhibitor Aromatic Interactions. *J. Med. Chem.* **2008**, *51* (17), 5264–5270.

(21) Young, T. S.; Young, D. D.; Ahmad, I.; Louis, J. M.; Benkovic, S. J.; Schultz, P. G. Evolution of Cyclic Peptide Protease Inhibitors. *P. Natl. Acad. Sci. USA* **2011**, *108* (27), 11052–11056.

(22) Hanna, R. A.; Garcia-Diaz, B. E.; Davies, P. L. Calpastatin Simultaneously Binds Four Calpains with Different Kinetic Constants. *FEBS Lett.* **2007**, *581* (16), 2894–2898.

(23) Venkatraman, S.; Njoroge, F. G. Macrocyclic Inhibitors of HCV NS3 Protease. *Expert Opin. Ther. Pat.* **2009**, *19* (9), 1277–1303.

(24) Abell, A. D.; Jones, M. A.; Coxon, J. M.; Morton, J. D.; Aitken, S. G.; McNabb, S. B.; Lee, H. Y.-Y.; Mehrtens, J. M.; Alexander, N. A.; Stuart, B. G.; Neffe, A. T.;

Bickerstaffe, R. Molecular Modeling, Synthesis, and Biological Evaluation of Macrocyclic Calpain Inhibitors. *Angew. Chem. Intl. Ed.* **2009**, *48* (8), 1455–1458.

(25) Donkor, I. O. A Survey of Calpain Inhibitors. *Curr. Med. Chem.* **2000**, *7* (12), 1171–1188.

(26) Donkor, I. O. Calpain Inhibitors: A Survey of Compounds Reported in the Patent and Scientific Literature. *Expert Opin. Ther. Pat.* **2011**, *21* (5), 601–636.

(27) Cuerrier, D.; Moldoveanu, T.; Campbell, R. L.; Kelly, J.; Yoruk, B.; Verhelst, S. H. L.; Greenbaum, D.; Bogyo, M.; Davies, P. L. Development of Calpain-Specific Inactivators by Screening of Positional Scanning Epoxide Libraries. *J. Biol. Chem.* **2007**, *282* (13), 9600–9611.

(28) Tripathy, R.; Ator, M. A.; Mallamo, J. P. Calpain Inhibitors Based on the Quiescent Affinity Label Concept: High Rates of Calpain Inactivation with Leaving Groups Derived From N-Hydroxy Peptide Coupling Reagents. *Bioorg. Med. Chem. Lett.* **2000**, *10* (20), 2315–2319.

(29) Siklos, M.; BenAissa, M.; Thatcher, G. R. J. Cysteine Proteases as Therapeutic Targets: Does Selectivity Matter? A Systematic Review of Calpain and Cathepsin Inhibitors. *Acta Pharm. Sin. B* **2015**, *5* (6), 506–519.

(30) Donkor, I. O. An Updated Patent Review of Calpain Inhibitors (2012 – 2014). *Expert Opin. Ther. Pat.* **2014**, 2*5* (1),1–15.

(31) Fukiage, C.; Azuma, M.; Nakamura, Y.; Tamada, Y.; Nakamura, M.; Shearer, T. R. SJA6017, A Newly Synthesized Peptide Aldehyde Inhibitor of Calpain: Amelioration of Cataract in Cultured Rat Lenses. *BBA - Mol. Basis Dis.* **1997**, *1361* (3), 304–312.

(32) Inoue, J.; Nakamura, M.; Cui, Y.-S.; Sakai, Y.; Sakai, O.; Hill, J. R.; Wang, K. K. W.;

Yuen, P.-W. Structure−Activity Relationship Study and Drug Profile of N-(4-Fluorophenylsulfonyl)- L-Valyl- L-Leucinal (SJA6017) as a Potent Calpain Inhibitor. *J. Med. Chem.* **2003**, *46* (5), 868–871.

(33) Tyndall, J. D. A.; Nall, T.; Fairlie, D. P. Proteases Universally Recognize Beta Strands in Their Active Sites. *Chem. Rev.* **2005**, *105* (3), 973–1000.

(34) Tyndall, J. D. A.; Fairlie, D. Macrocycles Mimic the Extended Peptide Conformation Recognized by Aspartic, Serine, Cysteine and Metallo Proteases. *Curr. Med. Chem.* **2001**, *8* (8), 893–907.

(35) Driggers, E. M.; Hale, S. P.; Lee, J.; Terrett, N. K. The Exploration of Macrocycles for Drug Discovery - An Underexploited Structural Class. *Nat. Rev. Drug Discov.* **2008**, *7* (7), 608–624.

(36) Yudin, A. K. Macrocycles: Lessons From the Distant Past, Recent Developments, and Future Directions. *Chem. Sci.* **2015**, *6* (1), 30–49.

(37) Marsault, E.; Peterson, M. L. Macrocycles Are Great Cycles: Applications, Opportunities, and Challenges of Synthetic Macrocycles in Drug Discovery. *J. Med. Chem.* **2011**, *54* (7), 1961–2004.

(38) Elce, J. S.; Hegadorn, C.; Gauthier, S.; Vince, J. W.; Davies, P. L. Recombinant Calpain II: Improved Expression Systems and Production of a C105A Active-Site Mutant for Crystallography. *Protein Eng. Des. and Sel.* **1995**, *8* (8), 843–848.

(39) Zaretsky, S.; Scully, C. C. G.; Lough, A. J.; Yudin, A. K. Exocyclic Control of Turn Induction in Macrocyclic Peptide Scaffolds. *Chem. Eur. J.* **2013**, *19* (52), 17668–17672.

(40) Morin, A.; Eisenbraun, B.; Key, J.; Sanschagrin, P. C.; Timony, M. A.; Ottaviano, M.; Sliz, P. Collaboration Gets the Most Out of Software. *eLife Sciences* **2013**, *2*, 2e01456.

(41) Hess, B.; Kutzner, C.; van der Spoel, D.; Lindahl, E. GROMACS 4: Algorithms for Highly Efficient, Load-Balanced, and Scalable Molecular Simulation. *J. Chem. Theory Comput.* **2008**, *4* (3), 435–447.

(42) Bjelkmar, P.; Larsson, P.; Cuendet, M. A.; Hess, B.; Lindahl, E. Implementation of the CHARMM Force Field in GROMACS: Analysis of Protein Stability Effects From Correction Maps, Virtual Interaction Sites, and Water Models. *J. Chem. Theory Comput.* **2010**, *6* (2), 459–466.

(43) Jorgensen, W. L.; Maxwell, D. S.; Tirado-Rives, J. Development and Testing of the OPLS All-Atom Force Field on Conformational Energetics and Properties of Organic Liquids. *J. Am. Chem. Soc.* **1996**, *118* (45), 11225–11236.

(44) Malde, A. K.; Zuo, L.; Breeze, M.; Stroet, M.; Poger, D.; Nair, P. C.; Oostenbrink, C.; Mark, A. E. An Automated Force Field Topology Builder (ATB) and Repository: Version 1.0. *J. Chem. Theory Comput.* **2011**, *7* (12), 4026–4037.

(45) Humphrey, W.; Dalke, A.; Schulten, K. VMD: Visual Molecular Dynamics. *J. Mol. Graph.* **1996**, *14* (1), 33–38.

(46) Morris, G. M.; Huey, R.; Lindstrom, W.; Sanner, M. F.; Belew, R. K.; Goodsell, D. S.; Olson, A. J. AutoDock4 and AutoDockTools4: Automated Docking with Selective Receptor Flexibility. *J. Comput. Chem.* **2009**, *30* (16), 2785–2791.

(47) Halgren, T. A.; Murphy, R. B.; Friesner, R. A.; Beard, H. S.; Frye, L. L.; Pollard, W. T.; Banks, J. L. Glide: A New Approach for Rapid, Accurate Docking and Scoring. 2. Enrichment Factors in Database Screening. *J. Med. Chem.* **2004**, *47* (7), 1750–1759.

(48) Friesner, R. A.; Banks, J. L.; Murphy, R. B.; Halgren, T. A.; Klicic, J. J.; Mainz, D. T.; Repasky, M. P.; Knoll, E. H.; Shelley, M.; Perry, J. K.; Shaw, D. E.; Francis, P.;

Shenkin, P. S. Glide: A New Approach for Rapid, Accurate Docking and Scoring. 1. Method and Assessment of Docking Accuracy. *J. Med. Chem.* **2004**, *47* (7), 1739–1749.

(49) Friesner, R. A.; Murphy, R. B.; Repasky, M. P.; Frye, L. L.; Greenwood, J. R.; Halgren, T. A.; Sanschagrin, P. C.; Mainz, D. T. Extra Precision Glide: Docking and Scoring Incorporating a Model of Hydrophobic Enclosure for Protein−Ligand Complexes. *J. Med. Chem.* **2006**, *49* (21), 6177–6196.

(50) Jacobson, M. P.; Friesner, R. A.; Xiang, Z.; Honig, B. On the Role of the Crystal Environment in Determining Protein Side-Chain Conformations. *J. Mol. Biol.* **2002**, *320* (3), 597–608.

(51) Jacobson, M. P.; Pincus, D. L.; Rapp, C. S.; Day, T. J. F.; Honig, B.; Shaw, D. E.; Friesner, R. A. A Hierarchical Approach to All-Atom Protein Loop Prediction. *Proteins* **2004**, *55* (2), 351–367.

(52) Kakkar, T.; Boxenbaum, H.; Mayersohn, M. Estimation of Ki in a Competitive Enzyme-Inhibition Model: Comparisons Among Three Methods of Data Analysis. *Drug Metab. Dispos.* **1999**, *27* (6), 756–762.

(53) Williams, T.; Kelley, C. Gnuplot 4.6: An Interactive Plotting Program. **2012**. http://gnuplot.sourceforge.net/

(54) Liu, Y.; Kati, W.; Chen, C.-M.; Tripathi, R.; Molla, A.; Kohlbrenner, W. Use of a Fluorescence Plate Reader for Measuring Kinetic Parameters with Inner Filter Effect Correction. *Anal. Biochem.* **1999**, *267* (2), 331–335.

(55) Zaretsky, S.; Tan, J.; Hickey, J. L.; Yudin, A. K. Macrocyclic Templates for Library Synthesis of Peptido-Conjugates. In *Computational Drug Discovery and Design*; Baron, R., Ed.; Methods in Molecular Biology; Springer New York: New York, NY, 2014; Vol.

1248, pp 67–80.

(56) O'Neil, K. T.; Erickson-Viitanen, S.; DeGrado, W. F. Photolabeling of Calmodulin with Basic, Amphiphilic Alpha-Helical Peptides Containing P-Benzoylphenylalanine. *J. Biol. Chem.* **1989**, *264* (24), 14571–14578.

(57) O'Neil, K. T.; DeGrado, W. F. The Interaction of Calmodulin with Fluorescent and Photoreactive Model Peptides: Evidence for a Short Interdomain Separation. *Proteins* **1989**, *6* (3), 284–293.

(58) Hili, R.; Rai, V.; Yudin, A. K. Macrocyclization of Linear Peptides Enabled by Amphoteric Molecules. *J. Am. Chem. Soc.* **2010**, *132* (9), 2889–2891.

(59) Zaretsky, S.; Hickey, J. L.; Tan, J.; Pichugin, D.; St. Denis, M. A.; Ler, S.; Chung, B. K. W.; Scully, C. C. G.; Yudin, A. K. Mechanistic Investigation of Aziridine Aldehyde-Driven Peptide Macrocyclization: The Imidoanhydride Pathway. *Chem. Sci.* **2015**, *6* (10), 5446–5455.

(60) Chou, J. S.; Impens, F.; Gevaert, K.; Davies, P. L. M-Calpain Activation in Vitro Does Not Require Autolysis or Subunit Dissociation. *BBA - Proteins Proteom.* **2011**, *1814* (7), 864–872.

(61) Betts, R.; Anagli, J. The β- and γ-CH2 of B27-WT's Leu11 and Ile18 Side Chains Play a Direct Role in Calpain Inhibition. *Biochemistry* **2004**, *43* (9), 2596–2604.

(62) Jo, H.; Meinhardt, N.; Wu, Y.; Kulkarni, S.; Hu, X.; Low, K. E.; Davies, P. L.; DeGrado, W. F.; Greenbaum, D. C. Development of A-Helical Calpain Probes by Mimicking a Natural Protein–Protein Interaction. *J. Am. Chem. Soc.* **2012**, *134* (42), 17704–17713.

(63) Yung-Chi, C.; Prusoff, W. H. Relationship Between the Inhibition Constant (KI) and the

Concentration of Inhibitor Which Causes 50 Per Cent Inhibition (I50) of an Enzymatic Reaction. *Biochem. Pharmacol.* **1973**, *22* (23), 3099–3108.

(64) Burlingham, B. T.; Widlanski, T. S. An Intuitive Look at the Relationship of Ki and IC50: A More General Use for the Dixon Plot. *J. Chem. Educ.* **2003**, *80* (2), 214.

(65) Cooper, A.; Dryden, D. T. F. Allostery Without Conformational Change. *Eur. Biophys. J.* **1984**, *11* (2), 103–109.

(66) Motlagh, H. N.; Wrabl, J. O.; Li, J.; Hilser, V. J. The Ensemble Nature of Allostery. *Nature* **2014**, *508* (7496), 331–339.

(67) Low, K. E.; Karunan Partha, S.; Davies, P. L.; Campbell, R. L. Allosteric Inhibitors of Calpains: Reevaluating Inhibition by PD150606 and LSEAL. *BBA - Gen. Subjects* **2014**, *1840* (12), 3367–3373.

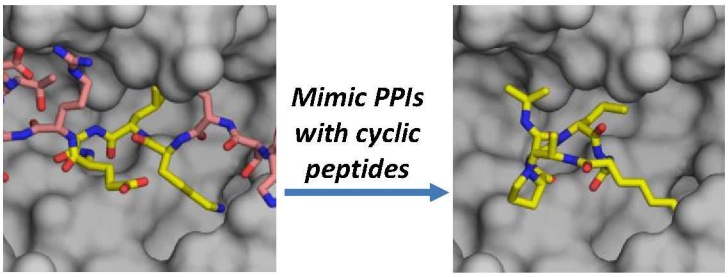
Mimic PPIs
with cyclic
peptides